Determination of Calcium Binding Sites in Gas-Phase Small Peptides by Tandem Mass Spectrometry

Olga V. Nemirovskiy and Michael L. Gross
Chemistry Department, Washington University, St. Louis, Missouri, USA

Low-energy (LE) and high-energy (HE) collisionally activated decompositions (CAD) of calcium/peptide complexes of the form $[M - H + Ca]^+$ and $[M + Ca]^{2+}$ reflect the site of calcium binding in various gas-phase peptides that are models of the calcium binding site III of rabbit skeletal troponin C. The Ca^{2+} binding sites involve an aspartic acid, glutamic acid, and asparagine, which are in the metal-binding loops of calcium-binding proteins. Both fast atom bombardment (FAB) and electrospray ionization (ESI) were used to generate the metal/peptide complexes. When submitted to LE CAD, ESI-produced Ca^{2+}/peptide complexes undergo fragmentations that are controlled by Ca^{2+} binding and provide information on the Ca^{2+} binding site. The LE CAD spectra are simple, indicating that Ca^{2+} binding involves specific oxygen ligands including acidic side chains and that only a few low-energy fragmentation channels exist. The HE CAD spectra of FAB-produced Ca^{2+}/peptide complexes are more complex, owing to the introduction of high internal energy into the precursor ion. Interactions of the other alkaline-earth metal ions Mg^{2+} and Ba^{2+} with these peptides reveal that the ligand preferences of these metal ions are slightly different than those of Ca^{2+}. (J Am Soc Mass Spectrom 1998, 9, 1020–1028) © 1998 American Society for Mass Spectrometry

Metal ions play a vital role in many biological processes. They act by triggering mechanisms, stabilizing structure, and controlling redox behavior [1, 2]. Of all the divalent metallic cations in the periodic table, calcium plays the most important role in biology. It acts as a secondary messenger in regulating numerous intracellular events, taking advantage of its large membranous concentration gradient. Mediation of cellular processes by Ca^{2+} ions involves calcium-binding proteins [3–7]. Various sites in these proteins vary greatly in their affinities for calcium depending on amino-acid sequence of the binding site [8]. The calcium affinities of small peptides with amino-acid sequences that are models of Ca^{2+} binding sites in proteins were previously studied in solution [9–11], and the results show that affinities are modulated by solvent effects. One motivation for extending these efforts to the gas phase is that comparison with solution properties brings understanding of solvent effects. Furthermore, metal-binding sites in interiors of proteins are hydrophobic, and interactions in the gas phase are an appropriate model for those in hydrophobic regions [1, 12].

For calcium-binding proteins, the portion that interacts with Ca^{2+} is part of a segment of 12 amino-acid residues that comprise the polypeptide loop between the helices [12–14]. The interacting ligands are at relative positions 1, 3, 5, 7, 9, and 12 of the loop and generally are carbonyl, carboxyl, and nonaromatic oxygens (e.g., from the side chains of Asp, Asn, Glu, Ser, and Thr). The calcium binding site III in rabbit skeletal troponin C has the sequence DRNADG as a part of the Ca^{2+} binding loop. The x-ray structure of this binding site reveals that side chains of residues at position 1 (D), 3 (N), and 5 (D) are involved in binding to Ca^{2+} [14].

The goal of our research is to determine by means of mass spectrometry the metal-binding sites in small gas-phase peptides that are models for the amino-acid sequence in large metal-binding proteins. Therefore, we chose small peptides that are models for Ca^{2+}-binding loops in proteins. We also used the same peptides to study their intrinsic affinities to calcium, and a description of this work will be published elsewhere [8]. To determine the important calcium-binding amino acids and their positions in a peptide chain, low-energy (LE) and high-energy (HE) collisionally activated decompositions (CAD) were followed for calcium/peptide complexes introduced into the mass spectrometer as $[M - H + Ca]^+$ and $[M + Ca]^{2+}$. The Ca^{2+}-containing monopositive ions were produced by fast atom bombardment (FAB) or electrospray ionization (ESI), whereas complexes of the neutral peptide with the divalent metal ion require ESI [15, 16]. We also describe interactions of the alkaline-earth metal ions Mg^{2+} and Ba^{2+}

Address reprint requests to Dr. M. L. Gross, Chemistry Department, Washington University, One Brookings Drive, Campus Box 1134, St. Louis, MO 63130. E-mail: MGross@wuchem.wustl.edu

1044-0305/98/$19.00
PII S1044-0305(98)00071-3

Received February 13, 1998
Revised April 29, 1998
Accepted May 11, 1998

with the peptides and compare the results with those involving Ca^{2+}.

In previous reports of intrinsic interactions of alkaline-earth metal ions and peptides, emphasis was given to opportunities for sequencing and for examining general interactions but not for investigating peptides that are models for binding in solution [17–19]. Other previous studies of alkaline-earth metal ions were of triply deprotonated tripeptides [20, 21] and showed that the interactions are strong and that the fragmentations characterize the amino acids at the N terminus.

Experimental

Reagents

The peptides used for this work were synthesized at the Washington University, Department of Pathology by automatic, stepwise, solid-phase peptide synthesis using Fmoc-protected amino acids. The crude peptides were released from the resin by ammonolysis, to give a C-terminal amidated species and purified by reverse-phase high-performance liquid chromatography (HPLC) using a C-18 column, and fractions were collected and lyophilized. The identity of the peptides was confirmed by FAB mass spectrometry and tandem mass spectrometry of the $[M + H]^+$ ions.

The cation-exchange resins (AG 50W-X8, mesh size: 200–400 μm) were purchased from the Bio-Rad Laboratories (Hercules, CA) in the H form. Conversion to Ca^{2+}-saturated resins was achieved by washing the H form with five-bed volumes of ~8 M calcium acetate. Any residual $Ca(OAc)_2$ solution was washed out by flushing the resin with three-bed volumes of deionized water (10^{18} Ω cm) [22].

Instrumentation

Mass spectrometric experiments were performed on a VG ZAB-T (Manchester, UK) four-sector and a Finnigan LCQ (San Jose, CA) ion-trap mass spectrometer. The former consisted of two-high mass, double-focusing mass spectrometers of BEBE design. The instrument was operated at an accelerating voltage 8 kV, and FAB was accomplished with Cs^+ ions from a gun that provided a 22-keV Cs^+ beam (the overall energy for desorption was 30 kV). FAB mass spectra were acquired by using the first stage (MS-1) at a mass resolving power of approximately 1200 (10% valley depth). The second stage (MS-2), which was a reverse-geometry, Mattauch–Herzog type instrument with a planar electrostatic analyzer, was used to obtain product-ion mass spectra after selecting the precursor ions with MS-1 and activating them by collisions in a cell containing helium gas at pressures sufficient to give 50% main-beam suppression. The fragment ions formed in the third-field-free region were detected by a single-point detector. The collision cell was floated at 4 kV.

For HE CAD of ESI-produced $[M + Ca]^{2+}$ ions, the VG-ZAB-T instrument was equipped with a VG ESI source. The ESI needle was at 8120 V, the sampling cone at 4200 V, and the ring electrode at 4120 V. Nitrogen was used as a bath and nebulizer gas at flow rates of 400 and 12 L/h, respectively. Sufficient peptide was dissolved in 80/20 water/methanol containing 0.1 mM calcium acetate to give a final concentration of 20 μM, and the solutions was continuously infused to the needle by using a Harvard model 22 syringe pump (Harvard Apparatus, South Natick, MA) at a flow rate 10 μL/min. In tandem mass spectrometry (MS/MS) experiments, fragment ions were collected on an array detector. Data acquisition was carried out with a VG OPUS V 3.1X data system, which was interfaced to the mass spectrometer by a VG SIOS I unit.

LE CAD experiments were carried out with a Finnigan LCQ ion-trap mass spectrometer equipped with an electrospray-ionization source. All samples were introduced at a flow rate of 10 μL/min. The spray needle was held at 4.2 kV, and a 4.4×10^5 Pa coaxial flow of nitrogen was used to stabilize the spray. A heated (200°C) stainless steel capillary served as the counterelectrode and was held at 13.5 V. In all experiments, helium was introduced to a pressure of 1 mtorr (measured by a remote ion gauge) for improving the trapping efficiency of the ion trap. The background helium gas also served as the collision gas during the CAD event. Collisional activation of the ions, which were excited by a "tickle" voltage applied to the end caps (20 eV), proceeded via multiple, low-energy collisions with helium.

A typical experimental sequence consisted of ion-injection times of 100–300 ms, and ion detection using the mass-selective instability mode at a scan rate of 5000 u/s. Ions were detected at a 15-kV conversion dynode supported by a channeltron electron multiplier. A 80/20 mixture of water/methanol was used as the carrier solvent.

Results and Discussion

Formation of the Ca^{2+}/Peptide Complexes

Ca^{2+}/peptide complexes were produced by both FAB and ESI. To form the $[M - H + Ca]^+$ ions under FAB conditions, a 1-μL aliquot of a 1-μg/μL peptide solution was mixed with the 3-NBA matrix and several beads of calcium-saturated cation-exchange resin on a FAB sample probe [23]. Under ESI conditions, singly charged $[M - H + Ca]^+$ and doubly charged $[M + Ca]^{2+}$ ions were produced when a mixture of peptide and 0.1 mM calcium-acetate solution was sprayed in a 20:80 MeOH:H_2O solvent system; $[M + H]^+$ and $[M + 2H]^{2+}$ ions were also observed under these conditions. The relative abundances of these various ions depend on pH, the solvent composition, amino-acid sequence, and amino-acid type. We optimized the conditions for producing abundant Ca^{2+}/peptide ions. Basic conditions favor formation of singly charged $[M - H + Ca]^+$ ions because deprotonation of the peptide must be

Table 1. Major[a] fragment ions formed under LE CAD of ESI-produced $[M - H + Ca]^+$

	Loss of				Formation of (n =)									
Peptide	H_2O	$2H_2O$	NH_3	H_2O, NH_3	y^*_n	$y^*_n - H_2O$	z^*_n	$z^*_n - H_2O$	b^*_n	$b^*_n - H_2O$	c^*_n	$c^*_n - H_2O$	c_n	b_n
NRDADGV	s[b]	—	—	m	6, 5	5	—	—	5	—	—	—	2	—
GNRDADA	s	—	—	m	5	5	6	6	6	—	5	5	3	—
DRADNA	s	—	—	m	—	—	—	—	4	4	—	—	—	—
NRDAVD	s	—	—	m	5, 4	—	—	—	5	—	—	—	2	2
NRDDAV	s	—	—	m	5, 4	5	4	—	4	—	—	—	2	—
DANADG	s	—	—	m	—	—	4	4	5	—	4	—	—	—
DDRANV	s	—	—	m	—	—	5	5	—	—	4	4	—	—
NRDADA	s	—	—	m	5, 4	5	—	—	5	—	4	4	2	—
DENADG[c]	s	m		m	5	—	5	—	5, 3	—	4	—	—	—
NRNADG	—	—	m	m	5	—	4	4	—	—	4	—	—	—
NRDANG	—	—	m	w	5	—	4	—	5	—	4	4	—	—
RDADGV	s	w[b]	—	—	—	—	—	—	4	4	3	—	—	—
RDADA	s	w	—	—	4	—	—	—	4	—	4, 3	3	—	—
ANRDAD	m[b]	—	s	m	4	4	5	—	—	—	5	5	3	3

[a]Major ions have relative abundances >1%. Ion designations are, for example, $y^*_n = [y_n - 2H + Ca]^+$ or $b^*_n = [b_n - 2H + Ca]^+$, where *n* is specified in the table.
[b]Refers to ion abundances: s = strong, m = medium, and w = weak.
[c]$[x_3 - 2H + Ca]^+$ also formed.

promoted. Under neutral conditions (no acid or base added), production of doubly charged $[M + Ca]^{2+}$ ions is favored because preserving the peptide as a neutral species is required. Under acidic conditions, protonation of the peptide is a major process, competitive binding to Ca^{2+} is diminished, and production of protonated species is favored.

The amino-acid sequence in the peptides also influences the relative abundances of the ions. Incorporation of additional acidic residues (e.g., aspartic acid) in the peptide causes the $[M - H + Ca]^+$ and $[M + Ca]^{2+}$ ions to be more abundant at neutral pH than the $[M + H]^+$ and $[M + 2H]^{2+}$ ions, whereas for peptides in which an amino acid was changed from basic to neutral to acidic (e.g., from DRNADG to DANADG to DENADG), the abundances of $[M + H]^+$ and $[M + 2H]^{2+}$ ions decreased by a factor of approximately 30%, whereas the $[M - H + Ca]^+$ abundance increased tenfold and that of $[M + Ca]^{2+}$ increased by approximately 30%. Removal of basic residue (e.g., arginine) from the peptide sequence leads to elimination of a major protonation site, favoring deprotonation of the peptide and Ca^{2+} binding.

Low Energy CAD of ESI-Produced Ions

LE CAD of $[M - H + Ca]^+$ ions. Upon low-energy collisional activation, the Ca^{2+}/peptide complexes fragment to give remarkably simple spectra of product ions; most product ions observed under LE CAD are presented in Table 1. The principal fragmentation pathway is typically loss of water followed by the loss of ammonia or, in some case, vice versa. The simplicity of the spectra shows that only a few low-energy fragmentation channels are open for the decomposition Ca^{2+}/peptide complexes, suggesting that there is strong binding between Ca^{2+} and a substantial portion of the peptide. For example, the calcium complex of peptide NRDADA (*m/z* 698) decomposes to give, besides major H_2O and NH_3 losses, small abundances of b^*_5, y^*_5, $[y^*_5 - H_2O]$, y^*_4, c^*_4, $[c^*_4 - H_2O]$ calcium-containing, and c_2 and b_2 noncalcium product ions (Figure 1). To keep the nomenclature of product ions simple, we omit the metal from the labels and designate product ions as if they were formed from protonated precursors; those ions that contain Ca^{2+} are designated by an $*$ in their labels. For example, a b^*_n ion is $[b_n - 2H + Cat]^+$, c^*_n is $[c_n - 2H + Cat]^+$, and y^*_n is $[y_n - 2H + Cat]^+$.

Product ions, which contain either the N or the C terminus, are formed by losses of residues comprised of only one or two amino acids, suggesting that the primary binding site for the Ca^{2+} is in the middle of the peptide (Scheme I for NRDADA). We amidated the C terminus to remove that carboxylate as a binding site. Thus, the anchor for Ca^{2+} binding is probably a deprotonated aspartic acid, but additional coordination by other amino-acid ligands stabilizes the complex. When C-terminal residues are involved in calcium coordina-

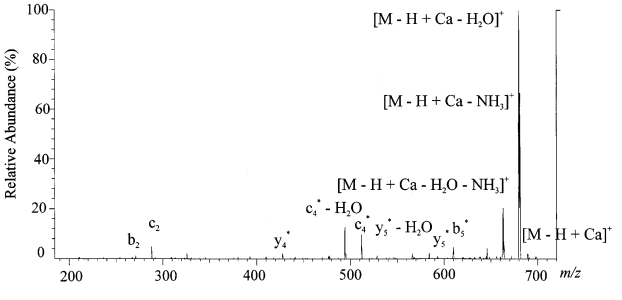

Figure 1. LE CAD spectrum of ESI-produced $[M - H + Ca]^+$ ion for Ca^{2+}/peptide complex of NRDADA.

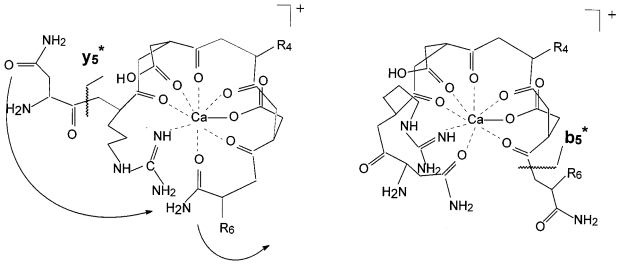

1 2

Scheme 1

tion (***1***, Scheme **1**), reactions near the N terminus will give y_n^* and z_n^* ions. On the other hand, b_n^* and c_n^* ions are formed when N-terminal residues coordinate the Ca^{2+}, leaving the C terminus free as a site of reaction (**2**, Scheme **1**). The y_n^*, z_n^*, b_n^*, and c_n^* sequence ions are favored, whereas a_n^* and other ions from side-chain cleavages do not form upon low-energy CA of calcium/peptide complexes. For some peptides, we observed y_n^* ions, for some z_n^* ions, and for some both. For example, the Ca^{2+}/DDRAVN complex does not give any y_n^* ions but instead produces a z_5^* ion. The Ca^{2+}/NRDAVD complex gives y_5^*, y_4^*, but no z_n^* ions, and Ca^{2+}/NRDDAV gives y_5^*, y_4^*, z_4^*, and no z_5^* (Table 1). To understand these fragmentations, we first propose structures of calcium-bound peptides and then consider mechanisms for precursor-ion decomposition.

For production of y_n^* ions, a proton may be transferred from either an α-carbon or an amide nitrogen of the preceding residue to another amide nitrogen via a five- or four-member ring as was proposed by Teesch and Adams [17]. An additional source of the needed proton in the peptides we studied is a neighboring aspartic-acid residue. That this proton can participate in the formation of a y_n^* ion was demonstrated by Beauchamp and co-workers [24] for a highly favored cleavage at aspartic-acid sites of $[pept + Na]^+$ ions. If this proton is removed upon binding to Ca^{2+}, then we

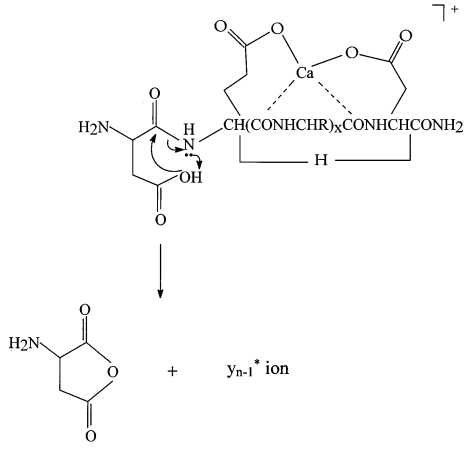

Scheme 2

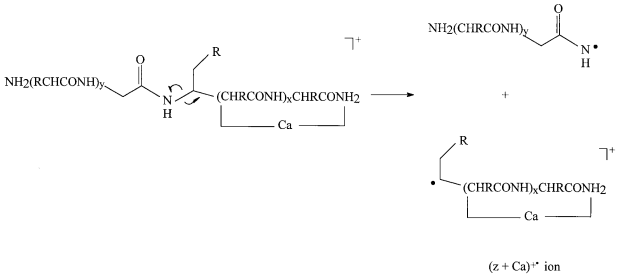

Scheme 3

would expect no y_{n-1}^* ions for peptides with Asp at the nth position from the C terminus. Examples that comply with this expectation are complexes of DDRANV, DANADG, and DRADNA, which give no y_5^* ion, and complexes of NRDADGV, DDRANV, and RDADGV, which give no y_4^* ions. An exception is DENADG, which gives an abundant y_5^* ion. This peptide contains three amino acids with acidic side chains, whereas those that give no y* contain only one or two. For the exception, we propose that Ca^{2+} is bonded, at least in part, to E and the D in position 2 from the C terminus, leaving the N-terminal D unbound to Ca^{2+} and with an available acidic proton to initiate cleavage to give y_5^* (see Scheme **2**). For the other peptides with two aspartic acids, both are involved in Ca^{2+} binding, precluding the H^+ transfer required to cleave the peptide bond and form the y_{n-1}^* ion.

Formation of z_n^* ions also depends on the amino-acid sequence of the peptides, and it is favored when cleavage takes place at aspartic-acid or asparagine residues. For example, the calcium complex of DANADG does not fragment to give a z_5^* ion, but does give a z_4^* ion, whereas DDRANV gives z_5^*, but not z_4^*. Teesch and Adams [17] reported that $z^{+\cdot}$ ions (a more complete description is $[z - H + Ca]^{+\cdot}$) can form from the precursor $[M - H + Ca]^+$ in which Ca^{2+} is bound to any site of the peptide chain. They proposed that the fragmentation giving $z^{+\cdot}$ product ions involves homolytic cleavage of the bond between the α-carbon and the amide nitrogen to give a distonic radical cation (Scheme **3**). The α-carboxy radical site is stabilized by the resonance delocalization with the carbonyl group of the

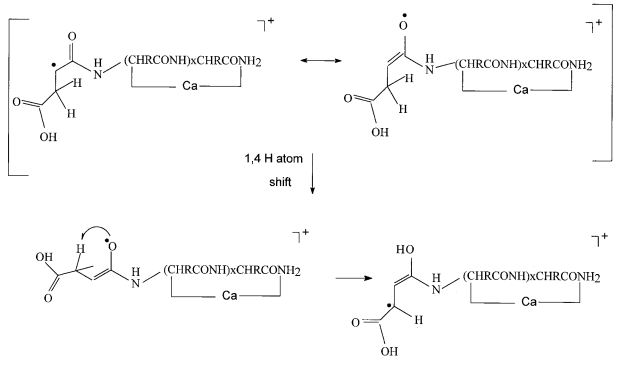

Scheme 4

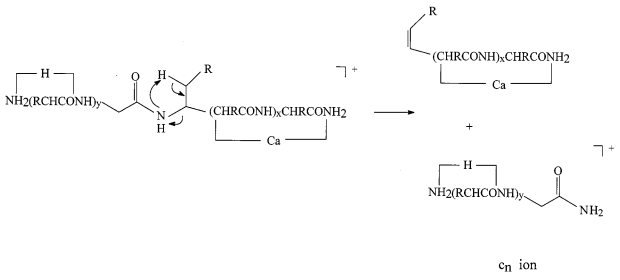

Scheme 5

peptide chain (Scheme IV). Because we observe $z^{+\cdot}$ ions from cleavage at residues containing carbonyl group in the side chain, we suggest that additional resonance stabilization of these distonic radical cation can occur. A 1,4-hydrogen atom shift interconverts the two resonance hybrids of the distonic radical cation (Scheme **4**).

Besides calcium-containing product ions, Ca^{2+}/peptide complexes give, when activated by low-energy collisions, unusual c_n and b_n ions, which do not contain Ca^{2+}. Hu and Loo [15] previously reported nonmetal-containing product ions from decomposition of $[peptide + Cat]^{2+}$, where Cat is a transition metal ion. Formation of ions without the Ca^{2+} requires elimination of a doubly negative peptide fragment containing the divalent calcium ion. The likely sites for double deprotonation are the carboxylic groups of the aspartic-acid side chains. Because the precursor is singly charged, a second deprotonation is necessary and may occur by the formation of a zwitterionic species containing a positive charge on the basic arginine residue and a negative charge on the carboxylic group of aspartic-acid residue. Therefore, we observe c_n ions that contain no calcium when the incipient product ion contains an arginine and no aspartic-acid residues. For example, the Ca^{2+}/peptide complex of NRDADGV gives a c_2 ion, whereas that of GNRDADA produces a c_3 ion (Table 1). The mechanism for the formation of the c_n ions requires bond breakage between the α-carbon and the amide nitrogen (Scheme **5**) and may proceed, as was suggested by Teesch and Adams [17], either by proton transfer from the β-carbon of the incipient neutral to the amide nitrogen of the incipient product ion, via a six-membered ring, or from the α-carbon to a distant amide nitrogen. The difference in the mechanism we propose (Scheme **5**) and that of Teesch and Adams [17] is that a metal ion is lost with the neutral, and charging of the fragment ion is by proton transfer. Sequential cleavage of c_n ions gives b_n ions. Appearance of small-mass, noncalcium-containing ions in LE CAD spectra of Ca^{2+}/peptide complexes is additional evidence that calcium binding is in the center of the peptide moiety.

LE CAD of $[M + Ca]^{2+}$ ions. Doubly charged $[M + Ca]^{2+}$ ions decompose upon multiple low-energy collisions in a fashion similar to that of their singly charged counterparts. The major fragmentations are losses of one or two water molecules and/or of ammonia (Table 2) to give doubly charged products. Although other fragmentations of the $[M + Ca]^{2+}$ ions give both singly and doubly charged products, there are no additional fragmentation channels for doubly charged $[M + Ca]^{2+}$ ions beyond those of singly charged $[M - H + Ca]^{+}$. For example, the $[M + Ca]^{2+}$ of NRDADA decomposes to give $[M - H_2O]^{2+}$, $[M - H_2O - NH_3]^{2+}$, y_4^*, $[y_4^* - H_2O]^{+}$, $[y_4^* - 2H_2O]^{+}$, $(b_5^*)^{2+}$, $(c_4^*)^{2+}$, $[c_4^* - H_2O]^{2+}$, c_2, and b_2 ions (Figure 2) in a pattern that is similar to that produced by the fragmentation of $[M - H + Ca]^{+}$. One obvious difference is that some fragment ions from

Table 2. Major[a] fragment ions formed under LE CAD of ESI-produced $[M + Ca]^{2+}$

	Loss of			Formation of (n =)													
Peptide	H_2O	$2H_2O$	H_2O, NH_3	y_n^*	$y_n^* - H_2O$[e]	$(y_n^*)^{2+}$	z_n^*	$z_n^* - H_2O$	$(z_n^*)^{2+}$	b_n^*	$b_n^* - H_2O$	$(b_n^*)^{2+}$	c_n^*	$c_n^* - H_2O$	$(c_n^*)^{2+}$	c_n	b_n
NRDADGV	s[d]	m	—	5	5	—	—	—	—	5	—	5	—	—	—	2	—
GNRDADA[b]	s	m	—	4	4	—	—	6	6	—	—	6	—	5	5	3	—
DRADNA	s	—	m	—	—	—	—	—	—	4	4	—	—	—	—	—	—
NRDAVD[c]	s	m	—	4	4	5	—	—	—	—	—	5	3	3	—	2	2
NRDDAV	s	m	—	4	4	—	—	—	—	—	—	—	—	—	—	3, 2	2
DANADG	m[d]	w[d]	—	4	—	5, 4	—	—	—	—	—	5	—	—	—	—	—
DDRANV	s	w		—	—	—	—	5	5	—	—	5	—	—	—	—	—
NRDADA	s	—	m	4	4	—	—	—	—	—	—	5	—	4	4	2	2
DENADG	m	—	—	—	—	5, 4	—	—	—	—	—	5	—	—	4	—	—
NRNADG	s	—	m	—	—	—	4	4	—	—	—	—	—	—	4	2	—
NRDANG	s	—	m	—	—	—	4	4	—	—	—	4	—	—	—	2	—
RDADGV	s	s	—	—	—	—	—	—	—	4	4	—	—	—	—	1	1
RDADA	s	m	—	4	4	—	—	—	—	—	—	—	—	—	—	1	1
ANRDAD	s	m	—	—	—	4	—	—	5	—	—	5	—	—	5	3	—

[a]Major ions have relative abundances > 1%. Singly charged ions do not have a charge-state designation in the symbol. Ion designations are, for example, $y_n^* = [y_n - 2H + Ca]^{+}$, $b_n^* = [b_n - 2H + Ca]^{+}$, and $(y_n^*)^{2+} = [y_n - H + Ca]^{2+}$, where n is specified in the table.
[b]$x_5^* - H_2O$ also formed.
[c]$(x_5^*)^{2+}$ also formed.
[d]Refers to ion abundances: s = strong, m = medium, and w = weak.
[e]$y_n^* - 2H_2O$ also formed.

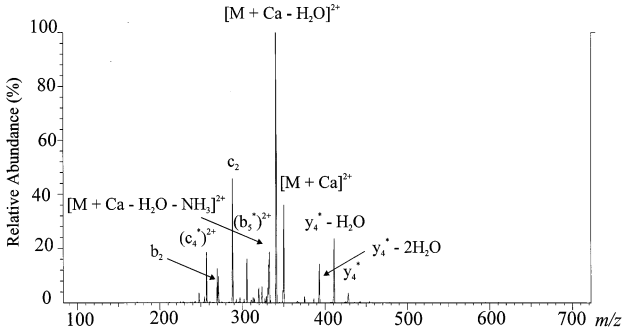

Figure 2. LE CAD spectrum of ESI-produced $[M + Ca]^{2+}$ ion for Ca^{2+}/peptide complex of NRDADA.

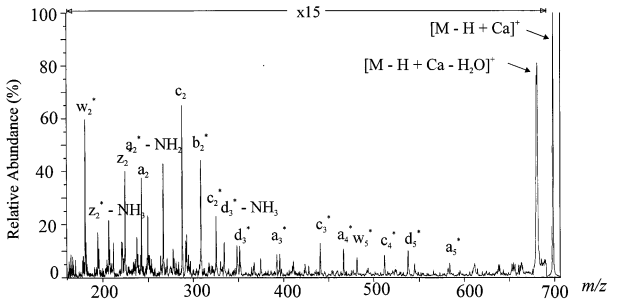

Figure 3. HE CAD spectrum of FAB-produced $[M - H + Ca]^+$ ion for Ca^{2+}/peptide complex of NRDADA.

$[M + Ca]^{2+}$ remain doubly charged, whereas no such ions are formed from $[M - H + Ca]^+$.

Some of the $[M + Ca]^{2+}$ ions were submitted to multiple stage decompositions (e.g., MS^3 and MS^4), and no unexpected decompositions of the Ca^{2+}/peptide complex were seen. Under MS^3 and MS^4, $[M + Ca - H_2O]^{2+}$ and $[M + Ca - H_2O - NH_3]^{2+}$ ions from NRDADA fragment by processes that are already faintly seen in the MS/MS experiment. The fragmentations of both $[M + Ca]^{2+}$ and $[M - H + Ca]^+$ suggest that the metal bonding in either the neutral or the deprotonated peptide is similar and that the metal ion interactions with the peptide are preserved upon LE CAD. All the calcium-containing fragment ions have aspartic-acid or asparagine residues, and that is consistent with the finding that these residues are important in calcium-binding loops of proteins.

Although a description of the behavior of $[M + H]^+$ and $[M + 2H]^{2+}$ ions is beyond the scope of this article, we make brief mention of it. LE CA of $[M + H]^+$ and $[M + 2H]^{2+}$ ions gives abundant water and/or ammonia losses, which are similar to the decomposition of $[M - H + Ca]^+$ and $[M + Ca]^{2+}$ ions. The most common ions formed upon LE CA of $[M + H]^+$ and $[M + 2H]^{2+}$, however, are a reasonably complete series of b_n and y_n ions but no c_n and z_n ions.

HE CAD of FAB and ESI-Produced Ions

HE CAD of FAB-Produced Ions. Under high-energy collisional activation, $[M - H + Ca]^+$ complexes decompose to give complicated mass spectra of products (Table 3). In contrast to LE CAD of ESI-produced ions, HE CA of FAB-produced ions gives a series of a^*_n, d^*_n, w^*_n, and v^*_n sequence ions. For example, the Ca^{2+} complex of NRDADA gives a facile water loss and a nearly complete series of a* and c* ions (no a^*_1 and c^*_1 were seen because the mass range for data acquisition was not set sufficiently low), d^*_3 and d^*_5 (related to the position of aspartic-acid residues), and some b^*_n, z^*_n, and w^*_n ions (Figure 3). Ions that do not contain Ca^{2+}, c_2 ions, also form under HE CA.

That the HE CAD mass spectra for alkaline-earth metal ion complexes of peptides with aliphatic amino acids are complicated is consistent with reports by

Table 3. Major[a] fragment ions formed under HE CAD of FAB-produced $[M - H + Ca]^+$

Peptide	Loss of H_2O	Formation of (n =)								
		x^*_n	y^*_n	z^*_n	a^*_n	b^*_n	c^*_n	d^*_n	c_n	y_n
NRDADGV	s[b]	—	5	5	4, 3, 2	2	2	5, 3	2	—
GNRDADA	m[b]	—	—	—	5, 2	—	6, 2	—	3	—
DRADNA	m	—	—	2	5	4	3	5, 4, 3	—	—
NRDAVD	m	5	—	3	4, 3, 2	2	5, 3	5	2	—
NRDDAV	s	3	3	4, 3	5, 4, 2[d]	3, 2	—	4, 3	2	5
DANADG	m	—	—	4[c]	—	3, 2	4, 2	5	—	—
DDRANV	m	—	5, 4, 3, 2	4	5, 4, 3, 2	5, 4	4, 3, 2	5	—	—
NRDADA	m	5	—	2	5, 4, 3, 2	2	4, 3, 2	5	2	5
DENADG	m	—	—	—	—	—	—	—	—	—
NRNADG	m	—	—	—	—	—	4, 2	—	—	—
RDADGV	m	—	4, 3, 2	—	4, 3, 2[d]	4, 3, 2, 1	—	—	1	—
RDADA	m	2	4	3, 2	—	1	1	4, 3	1	—
ANRDAD	s	5, 2	—	5	—	—	—	4, 3	5, 3	—

[a]Major ions have relative abundances > 1%. Singly charged ions do not have a charge-state designation in the symbol. Ion designations are, for example, $y^*_n = [y_n - 2H + Ca]^+$ *and* $(y^*_n)^{2+} = [y_n - H + Ca]^{2+}$, *where* n is specified in the table.
[b]Refers to ion abundances: s = strong, m = medium, and w = weak.
[c]$z^*_4 - H_2O$ also formed.
[d]$a^*_2 - NH_2$ also formed.

Table 4. Major[a] fragment ions formed under HE CAD of ESI-produced $[M + Ca]^{2+}$

	Loss of			Formation of (n =)													
Peptide	H_2O	NH_3	46	x^*_n	$(x^*_n)^{2+}$	y^*_n	$(y^*_n)^{2+}$	z^*_n	$(z^*_n)^{2+}$	a^*_n	$(a^*_n)^{2+}$	b^*_n	$(b^*_n)^{2+}$	c^*_n	$(c^*_n)^{2+}$	d^*_n	$(d^*_n)^{2+}$	w^*_n
NRDADGV	s[b]	m	m	—	—	—	—	—	6	—	5, 4	4	—	6	—	—	5	—
GNRDADA	m[b]	m	m	—	—	6	5	6	—	6	5, 4	4	6, 4	—	5	—	6, 4	—
DRADNA	m	m	m	—	—	—	—	—	—	—	5	—	5	—	5	—	—	—
NRDAVD	m	m	m	5	—	5	—	5	—	5, 4	—	—	—	—	—	5	—	—
NRDDAV	s	s	m	5	—	5	—	5	—	4	—	4	—	4	——	4	—	
DANADG	m	m	m	—	5, 4	—	5	—	5, 4	—	5	—	—	—	5	—	—	—
DDRANV	m	m	m	—		—	—	—	—	—	5, 3	—	4	—	—	5	—	—
NRDADA	m	m	m	—	5	—	5	—	—	—	—	—	—	—	—	—	—	—
DENADG	m	m	m	—	—	—	4	—	—	—	5	—	5, 4	—	—	—	—	—
NRNADG	m	m	m	—	—	—	5	—	—	—	—	—	—	—	5, 4	—	—	—
NRDANG	m	m	m	—	—	—	5	—	—	—	5	—	4	—	—	—	—	—
RDADGV	m	m	m	—	—	—	—	—	—	—	5, 4	—	—	—	5	—	4	5, 4
RDADA	m	m	m	—	—	4	—	—	—	—	4	—	4	—	—	—	4	4
ANRDAD	s	m	m	—	—	5	—	5	—	—	4	—	—	—	4	—	—	4

[a]Major ions have relative abundances > 1%. Ion designations are, for example, $y^*_n = [y_n - 2H + Ca]^+$ or $b^*_n = [b_n - 2H + Ca]^+$, where n is specified in the table.
[b]Refers to ion abundances: s = strong, m = medium, and w = weak.

Teesch and Adams [17]. They suggested that the precursor ions exist as a mixture of isomeric structures; the peptides have more than one intrinsic metal-binding site, and these compete for the metal. The isomeric forms decompose to give a complicated pattern of fragment ions. The relative abundance of a particular product ion is determined by the stabilization of the binding site in the precursor. In another article, Adams and co-workers [18] reported that the metastable-ion decompositions of negatively charged alkaline-earth complexes of peptides containing functional side chains (Asp, Glu, Tyr, His, and Trp) show more specific binding. Nevertheless, the product-ion mass spectra are still complex.

The motivation for choosing the peptides investigated here is to provide a strong binding site for the Ca^{2+} and test the ability of collisional activation to probe the location of that site. Although we expected the strong intrinsic binding of Ca^{2+} to peptides that is revealed by LE CA, the extensive fragmentations that were observed upon HE CA were less expected. When high-energy collisions were used to activate ESI-produced $[M - H + Ca]^+$ ions, the same mass-to-charge ratio product ions arise as those formed from FAB-produced precursors, except they are produced at lower abundances. The internal energy of ions formed under FAB conditions and activated by HE CA is responsible for the extensive fragmentations. The appearance of c_n ions that do not contain Ca^{2+} in both LE and HE CAD spectra again is evidence that a fraction of the decomposing Ca^{2+}/peptide structures are similar to those interrogated by LE CAD. But additional structures are formed as a consequence of the greater energy deposited into the complex upon HE CA. This internal energy permits coordination of Ca^{2+} ions by multiple peptide sites and allows different sequence ions to form as the metal ion moves along the peptide chain. LE CA of ESI-produced ions, however, reveals more clearly the specificity of Ca^{2+} binding to these peptides.

HE CAD of ESI-produced $[M + Ca]^{2+}$ ions. Upon HE CA, $[M + Ca]^{2+}$ ions decompose differently than when submitted to LE CA. In addition to formation of singly and doubly charged a*, d*, w*, and v* ions (Table 4), losses of water and ammonia occur. Furthermore, new losses of H_2O and CO take place to give $[M + Ca - 46]^{2+}$ upon HE activation. Although most Ca^{2+}/peptide complexes do decompose to give sequence ions, the relatively large size ($n > 3$) of the fragments suggests that the complexation with the metal ion prevents more complete decomposition of the precursor ion. The neutral or charged fragments that are cleaved from the $[M + Ca]^{2+}$ ion are of small mass, leaving intact the preferred binding of Ca^{2+} to the peptide. For example, the doubly charged Ca^{2+}/peptide complex of NRDADA fragments upon HE CA to give $[M - H_2O + Ca]^{2+}$ of m/z 341, $[M - H_2O - CO + Ca]^{2+}$ of m/z 327, an abundant $(y^*_5)^{2+}$ of m/z 292, a $(z^*_5)^{2+}$ of m/z 285, and a w^*_2 of m/z 182 (Figure 4). The differences in fragmentation upon LE and HE CA of ESI-produced

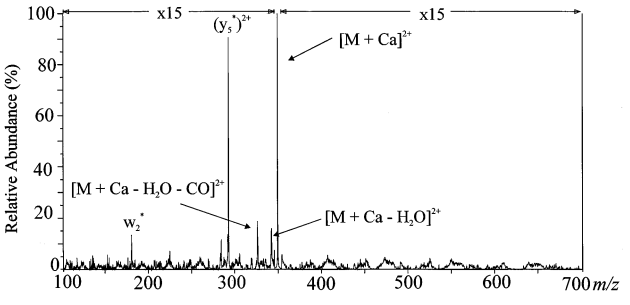

Figure 4. HE CAD spectrum of ESI-produced $[M + Ca]^{2+}$ ion for Ca^{2+}/peptide complex of NRDADA.

Table 5. Relative ion abundances for distinctive fragment ions for ESI-produced $[M + Cat]^{2+}$ of ANRDAD

Metal ion	Relative intensities of metal-containing ions, % $(c_5^*)^{2+}$	$(z_5^*)^{2+}$	Nonmetal ion, % c_3
Mg^{2+}	35	100	15
Ca^{2+}	70	45	40
Ba^{2+}	45	20	80

$[M + Ca]^{2+}$ ions are consistent with the concept that HE activation deposits more energy into the complexes, causing different and more extensive fragmentation to occur.

Comparison of LE CAD of Mg^{2+}, Ca^{2+}, and Ba^{2+}/Peptide Complexes

Although the types of fragmentations of metal/peptide complexes containing either Mg^{2+} or Ba^{2+} ions are nearly identical to those of complexes containing Ca^{2+}, the relative abundances depend on the nature of the metal ion. The trend in sizes of the metal ions is reflected in the relative ion abundances. The ionic radius of a Ba^{2+} ion with a given coordination number is greater than those of Ca^{2+} and Mg^{2+} with the same coordination number. For a given peptide sequence, the abundances of the specific N-terminal ions are high, intermediate, and low for Mg^{2+}, Ca^{2+}, and Ba^{2+}/peptide complexes, respectively, whereas the abundances of the specific C-terminal ions are reversed: high, intermediate, and low for Ba^{2+}, Ca^{2+}, and Mg^{2+}/peptide complexes, respectively. For example, the $[M + Mg]^{2+}$ of ANRDAD fragments to give very abundant $[z_5 - H + Mg]^{2+}$ ions and low-abundance $[c_5 - H + Mg]^{2+}$ and c_3 ions. On the other hand, decomposition of the Ba^{2+}/peptide complex gives low-abundance $[z_5 - H + Ba]^{2+}$ ions but abundant $[c_5 - H + Ba]^{2+}$ and c_3 ions (Table 5). A similar trend pertains to decompositions of metal/peptide complexes as $[M - H + Cat]^+$ ions (Table 6). When the peptide sequence is DRADNA, an N-terminal $[c_4 - 2H + Mg - H_2O]^+$ ion dominates, whereas an abundant C-terminal $[y_5 - 2H + Ba]^+$ ion characterizes the Ba^{2+}/peptide complex. Ca^{2+}/peptide complexes in both cases decompose to give ions whose abundances are intermediate to those of Mg^{2+} and Ba^{2+} complexes (Tables 5 and 6). The relative product-ion abundances depend on the binding preferences of different metal ions. Mg^{2+} acts as a hard acid, preferring hard-base ligands (e.g., deprotonated carboxylic acid groups of aspartates), whereas Ba^{2+} behaves as a softer acid, favoring softer carbonyl oxygen ligands and N-terminal nitrogen ligands. Ligand preferences of Ca^{2+} are intermediate; it is a harder acid than Ba^{2+} but softer than Mg^{2+}.

Table 6. Relative ion abundances for distinctive fragment ions for ESI-produced $[M - H + Cat]^+$ of ANRDAD

Metal ion	Relative intensities of metal-containing ions, % c_5^*	z_5^*	Nonmetal ion, % c_3
Mg^{2+}	10	100	15
Ca^{2+}	30	50	30
Ba^{2+}	60	10	20

Conclusion

ESI-produced Ca^{2+}/peptide complexes, when submitted to LE CA, undergo fragmentations that are determined by the location of the Ca^{2+} binding site. The nature and simplicity of the LE CAD spectra indicate that the binding of the Ca^{2+} ions to the peptide is to deprotonated acid side chains and to carbonyl oxygens. This binding involves a large fraction of the carbonyls of these small peptides, permitting only a few low-energy fragmentations that "trim" away the N- and/or C-termini portions, depending on the binding site of the peptide. The complexity of the HE CAD spectra of FAB-produced Ca^{2+}/peptide complexes shows that additional Ca^{2+} binding sites become populated when the complexes become more energized. Mg^{2+} and Ba^{2+} also interact with these peptides in a qualitatively similar way.

Acknowledgments

This work was supported by the National Institutes of Health, National Center for Research Resources (Grant No. P41RR00954). The authors wish to thank Professor E. Unanue of the Department of Pathology, Washington University Medical School for his support of the peptide syntheses.

References

1. (a) Hughes, M. N. *The Inorganic Chemistry of Biological Processes, 2nd ed.*; Wiley: New York, 1972; pp 1–50. (b) Berg, J. M. *Cold Spring Harbor Symp. Quant. Biol.* **1987,** *LII*, 579–585.
2. (a) Creighton, T. E. *Proteins: Structure and Molecular Properties, 2nd ed.*; Freeman; New York, 1993, p 507. (b) Bertini, I.; Gray, H. B.; Lippard, S. J.; Valentine, J. S. *Bioinorganic Chemistry*; University Science Book: Mill Valley, Ca, 1994; pp 107–166.
3. Baker, W. C.; Ketcham, L. K.; Dayhoff, M. O. In *Atlas of Protein Sequence and Structure*, Vol. 5; Dayhoff, M. O., Ed.; National Biomedical Research Foundation: Silver Spring, MD, 1965, pp 13–50.
4. Vogt, H. P.; Strassburger, W.; Wollmer, A.; Fleischhauer, J.; Bullard, B.; Mercola, D. *J. Theor. Biol.* **1979,** *76*, 297–310.
5. Reid, R. E.; Hodges, R. S. *J. Theor. Biol.* **1980,** *84*, 401–444.
6. Gariépy, J.; Hodges, R. S. *FEBS Lett.* **1983,** *160*, 1–6.
7. Crivici, A.; Ikura, M. *Annu. Rev. Biophys. Struct.* **1995,** *24*, 85–116.
8. Nemirovskiy, O. V.; Gross, M. L. *J. Am. Chem. Soc.*, submitted.
9. Marsden, B. J.; Hodges, R. S.; Sykes, B. D. *Biochemistry* **1988,** *27*, 4198–4206.

10. Marsden, B. J.; Hodges, R. S.; Sykes, B. D. *Biochemistry* **1989,** *28*, 8839–8847.
11. Shaw, G. S.; Hodges, R. S.; Sykes, B. D. *Biochemistry* **1991,** *30*, 8339–8347.
12. Kretsinger, R. H.; Nockolds, C. E. *J. Biol. Chem.* **1973,** *248*, 3313–3326.
13. Herrberg, O.; Moult, J.; James, M. N. G. *Methods Enzymol.* **1987,** *139*, 610–632.
14. Strydnaka, N. C. J.; James, M. N. G. *Annu. Rev. Biochem.* **1989,** *58*, 951–998.
15. Hu, P.; Loo, J. A. *J. Am. Chem. Soc.* **1995,** *117*, 11314–11319.
16. Loo, J. A.; Hu, P.; Smith, R. D. *J. Am. Soc. Mass Spectrom.* **1994,** *5*, 959–965.
17. Teesch, L. M.; Adams, J. *J. Am. Chem. Soc.* **1990,** *112*, 4110–4120.
18. Zhao, H.; Reiter, A.; Teesch, L. M.; Adams, J. *J. Am. Chem. Soc.* **1993,** *115*, 2854–2863.
19. Kückelmann, U.; Müller, D.; Weber, C. *J. Mol. Struct.* **1997,** *412*, 135–139.
20. Hu, P.; Gross, M. L. *J. Am. Chem. Soc.* **1992,** *114*, 9153–9160.
21. Hu, P.; Gross, M. L. *J. Am. Chem. Soc.* **1992,** *114*, 9161–9169.
22. *Guide to Ion Exchange*; BioRad Chem. Div., Bio Rad Lab., p. 6 Catalog Number 140-1997.
23. Vollmer, D. L.; Gross, M. L. *J. Mass Spectrom.* **1995,** *30*, 113–118.
24. Lee, S.-W.; Kim, H. S.; Beauchamp, J. L. *J. Am. Chem. Soc.* **1998,** *120*, 3188–3195.